IEEE Access
Multidisciplinary | Rapid Review | Open Access Journal

Date of publication xxxx 00, 0000, date of current version xxxx 00, 0000.

Digital Object Identifier 10.1109/ACCESS.2024.0429000

Variation in Photovoltaic Energy Rating and Underlying Drivers Across Modules and Climates

Kevin S. Anderson[1], Joshua S. Stein[1], and Marios Theristis[1]
[1]Sandia National Laboratories, Albuquerque, NM 87185, USA

Corresponding author: Kevin S. Anderson (e-mail: ksande@sandia.gov).

This work was supported by the U.S. Department of Energy's Office of Energy Efficiency and Renewable Energy (EERE) under the Solar Energy Technologies Office Award Numbers 38267 and 52788.

ABSTRACT The performance of photovoltaic (PV) modules is determined by the interplay between their inherent characteristics and the prevailing weather conditions. Although the impacts of different characteristics (e.g., low-light behavior, spectral mismatch, temperature coefficient, etc) are known, they have not been quantified over large geographic regions. This study uses the Climate Specific Energy Rating (CSER) and specific yield metrics as criteria to determine how different PV modules perform across climates in the contiguous United States (CONUS) and identifies the underlying drivers behind the observed variations. The annual CSER and specific yield of various PV technologies vary by more than 10% and 30%, respectively, across the CONUS. As expected, temperature has the most significant impact on CSER, affecting CSER by up to 13.1%, while spectral effects account for up to 4.9% variation in the case of cadmium telluride modules. Additionally, minor differences in parameter estimation procedures are shown to result in CSER differences of up to 1.5% in some climates. Furthermore, the IEC 61853-4 reference climatic datasets are found to overestimate CSER by 2–4% relative to climatic data for locations of actual PV systems in the United States. A new set of reference locations that accurately represents CSER across CONUS is proposed as an alternative to the IEC 61853-4 reference datasets.

INDEX TERMS performance, IEC 61853, modeling, spectrum, irradiance, temperature, incidence angle

I. INTRODUCTION

PHOTOVOLTAIC system energy yield depends on the interaction between system characteristics and local climate; any given system design is better suited to some climates than others. The primary source of this climatic dependence is that conversion efficiency varies with operating condition differently across module technologies. For example, it is well known that the conversion efficiency of thin-film cadmium telluride (CdTe) modules changes less with operating temperature than that of typical crystalline silicon (c-Si) modules. In addition to temperature, other influences on PV conversion efficiency include variation in angular response, spectral response, and absolute light intensity [1]. PV performance in any given climate will thus vary according to how the climate differs from standard test conditions (STC) in each of these dimensions (and with other factors like array design). This climatic variation motivates ''climate-specific energy rating'' (CSER) procedures to rate PV modules according to their energy output in various representative climates rather than merely their power at STC. One example is the CSER procedure specified in the IEC 61853-3 standard [2], [3].

The CSER is a means of combining the effects of individual aspects of PV performance (e.g. temperature and angular response) into a single metric reflecting a module's overall performance (relative to STC performance) under a particular set of realistic weather conditions. This combination of effects depends on both module and climate since not all climates differ from STC equally, nor do all modules respond to non-STC conditions similarly. This is demonstrated in Fig. 1, showing how the range of the effect of each of four performance aspects varies according to location and module. Performance effects that are important for a module in one location may be insignificant for a different location or module.

This climatic variation has been quantified for specific characteristics (e.g., temperature [4] and spectrum [5]–[10]), for specific locations [10]–[13], omitting some performance effects [14]–[16], or using generic PV module data [1], [17], but a comprehensive multi-characteristic climatic study using real module data has not been performed to date. Furthermore, although many studies have examined performance ratio (PR) [1], [4], [18]–[20] or performance loss rate (PLR)

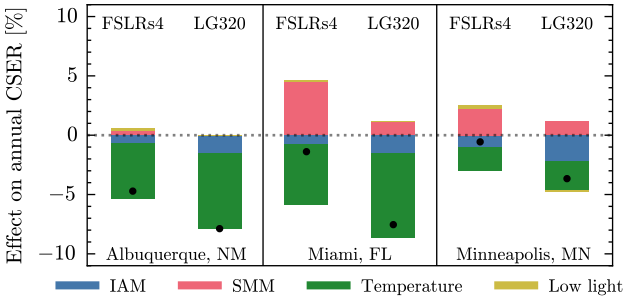

FIGURE 1. Climate-specific energy ratings (CSERs) for two modules and three locations, showing how various aspects of module performance contribute to the overall CSER, and how these contributions vary across locations and modules. IAM and SMM refer to the incidence angle modifier and spectral mismatch, respectively. Stacked bars above (below) zero indicate performance gain (loss) relative to STC. Black dots indicate the overall CSER. See Table 1 for interpretation of the module names.

[21], [22] variations across large geographic regions, there has been no such focus on CSER. While PR and PLR are widely used to assess PV system performance, they do not account for the specific interactions between PV technologies and local climatic conditions. In contrast, CSER provides a detailed view of how different module technologies perform under varying climate factors. Additionally, the sensitivity of CSER to uncertainty in performance modeling assumptions remains unclear. One study found that different estimation methods for thermal parameters resulted in up to 1% difference in CSER [23]. However, how this result generalizes to other technologies and estimation scenarios remains unexplored. Finally, it is unclear to what extent the IEC 61853-4 [24] reference climatic datasets represent climates in the contiguous United States (CONUS). These datasets are intended to standardize the evaluation of PV module performance, but the extent to which they reflect diverse climatic conditions has not been investigated besides a study in Freiburg, Germany where deviations up to 2.9% were found when compared against the CSER using the temperate continental dataset [25]. As such, quantification of CSER across diverse geographic regions remains largely unexplored. In this work, we investigate:

1) How do CSER and specific yield vary across the CONUS and a range of PV module technologies?
2) Which aspects of PV module performance are the primary sources of the CSER variation?
3) How does uncertainty in performance modeling parameter values affect estimated CSER?
4) How does CSER vary seasonally?
5) Are the IEC 61853-4 climatic datasets representative of the CONUS, and can we propose a better alternative?

This work is a part of PV Atlas, a project from the PV Performance Modeling Collaborative. The results of this study will be used for interactive maps on the PV Atlas website to facilitate solar energy education and support PV developers and other industry stakeholders. For more details, see the Data Availability section.

II. METHODS

A. CLIMATE DATASETS

CSER is evaluated using solar resource and meteorological data from the National Solar Radiation Database (NSRDB). We use 30-minute NSRDB data for approximately 21,000 locations on a 0.2° x 0.2° degree grid across the CONUS. The dataset corresponds to the calendar year 2022 and was generated from the NSRDB's Physical Solar Model, version 4.0.0 [26]. Each CONUS grid location is labeled with a Köppen-Geiger (KG) climate zone using the *kgcPy* package [27].

In addition to the base NSRDB dataset, we use a gridded dataset of spectral irradiance data corresponding to the same spatial and temporal grid as the NSRDB dataset. This dataset, representing global tilted spectral irradiance for 2002 wavelengths spanning 280–4000 nm, was simulated with the FARMS-NIT model [28], [29] assuming single-axis tracking with a ground coverage ratio of 0.3 and backtracking enabled. FARMS-NIT is noteworthy in that it is an all-sky model, meaning the spectra are computed accounting for cloud cover.

CSER computed for these gridded datasets are compared with CSER for the six reference climatic datasets in IEC 61853-4 [24]. These datasets are labeled "temperature continental", "temperature coastal", "subtropical coastal", "subtropical arid", "tropical humid", and "high elevation" and are provided for use with the IEC 61853-3 energy rating standard [2]. The standard states that these datasets are intended to be "representative of global regions relevant for the application of photovoltaics".

B. PV MODULE ENERGY RATING

We consider modules corresponding to five PV technologies: aluminum back surface field (Al-BSF), passivated emitter and rear cell (PERC), n-type passivated emitter and rear totally diffused (N-PERT), *silicon heterojunction (SHJ)*, and CdTe. These modules represent a diverse range of cell technologies in use today and their performance characterization datasets according to IEC 61853-1 and -2 are publicly available [30]–[33].

Table 1 presents characterization data for each module, including STC efficiency (η_{STC}), temperature coefficient of power (γ_{mp}), Faiman thermal coefficients (u_0 and u_1), and Martin/Ruiz IAM coefficient (a_r). Each module's efficiency, external quantum efficiency, and IAM profile are shown in Figs. 2 and 3.

Energy ratings for each module are calculated following the IEC 61853-3 standard [2] , which defines CSER as

$$\mathrm{CSER} = \frac{E_{sim}/H_p}{P_{stc}/G_{ref}}, \tag{1}$$

where E_{sim} is the simulated annual energy output of the module, H_p is the annual in-plane irradiation, P_{stc} is the maximum power under standard test conditions, and G_{ref} is the irradiance at standard test conditions. CSERs calculated according to this standard can be understood as the ratio of a

TABLE 1. Descriptions and characterization data for the PV modules considered in this work.

Name	Module	Cell type	η_{STC} [%]	γ_{mp} [%/°C]	u_0 $\left[\frac{W/m^2}{°C}\right]$	u_1 $\left[\frac{W/m^2}{°C\ (m/s)}\right]$	a_r [-]
CSmono275	Canadian Solar CS6K-275M	Al-BSF	16.9	-0.415	28.825	4.452	0.1524
Qmono300	Q Cells Q.PEAK-G4.1 300	PERC	17.4	-0.403	30.536	5.019	0.1553
LG320	LG 320 N1K-A5	N-PERT	18.7	-0.400	24.229	7.182	0.1590
Panasonic325	Panasonic VBHN325SA 16	*SHJ*	19.3	-0.297	24.614	7.878	0.1521
FSLRs4	First Solar FS-4112-3	CdTe	16.4	-0.297	24.4	6.904	0.1160

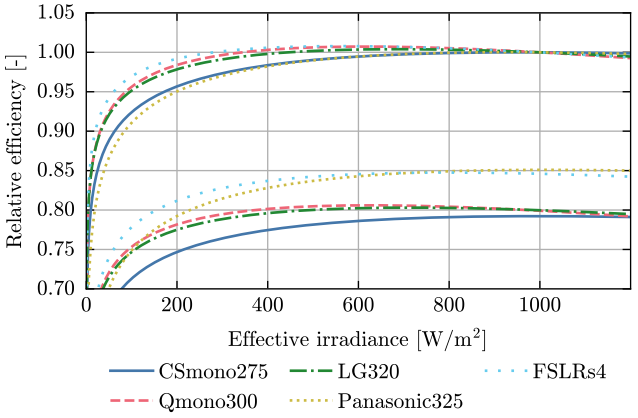

FIGURE 2. Relative efficiency profiles for the five modules fitted to test lab measurements at various irradiance and temperature conditions. Each profile is normalized to the module's efficiency at STC. The upper and lower groups of lines correspond to operating temperatures of 25°C and 75°C, respectively.

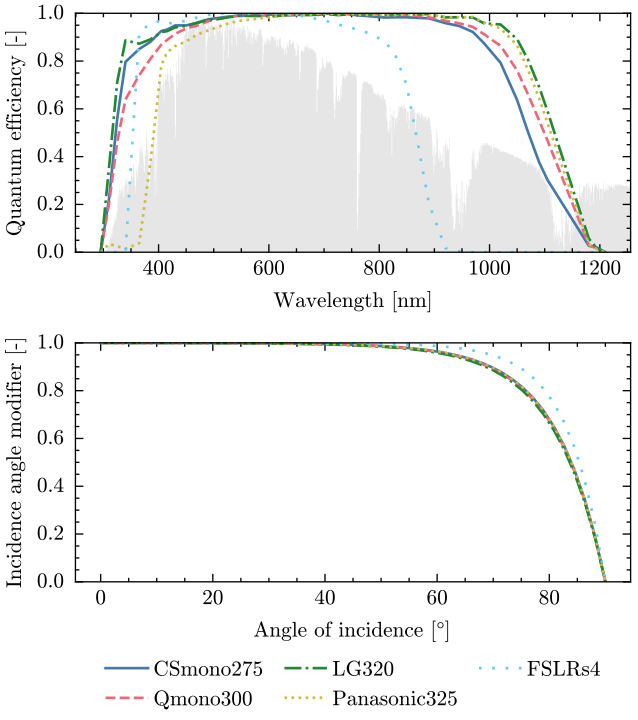

FIGURE 3. Each module's normalized external quantum efficiency (top) and incidence angle modifier profiles (bottom) from test lab characterization measurements. The shaded area indicates the AM 1.5G reference spectrum.

location-specific efficiency to the nominal efficiency at STC. The location-specific efficiency (E_{sim}/H_p) is determined by a modeling workflow that accounts for the effects of spectral variation, operating temperature, absolute irradiance level, and reflection loss. Each of these modeling steps is performed using the corresponding model implementations provided in the open-source PV modeling toolbox *pvlib-python* [34], [35], version 0.11.0 [36]. However, the energy rating procedure in this work differs slightly from the IEC 61853-3 method in the following ways:

1) Different climate datasets; i.e., all climates observed in CONUS instead of the IEC 61853-4 datasets
2) 30-minute climatic data instead of hourly
3) Higher-resolution spectra (FARMS-NIT provides 2002 spectral bands while IEC 61853-4 provides only 29)
4) Modeled global tilted irradiance (GTI) as it is not provided by the NSRDB
5) Single-axis tracking instead of fixed tilt
6) Performance modeling using the ADR model [37], [38] instead of bilinear interpolation, as interpolation is not fully specified [39].

The choice of single-axis tracking instead of fixed-tilt orientation was to better match large-scale PV systems deployed in the United States today, the large majority of which use single-axis trackers [40].

To investigate the underlying sources of variation in CSER, we also compute CSER values where individual performance effects are held at their STC values instead of varying according to the climatic dataset. For example, IAM is kept at STC by setting it to 1.0 for all angles of incidence. Four aspects of performance are evaluated in this way: IAM, spectral mismatch (SMM), low-light response, and temperature response. By computing CSER values with each of these effects "disabled" (i.e., held at the corresponding STC condition) and comparing with the baseline CSER where all effects are active, we can quantify each effect's share of the overall variation in CSER.

We also calculate a second metric, the specific yield. This metric represents the module's annual energy production, normalized to its nameplate power rating:

$$\text{Specific Yield} = \frac{E_{sim}}{P_{stc}} = \text{CSER} \cdot \frac{H_p}{G_{ref}} \tag{2}$$

In other contexts, specific yield is typically calculated considering a complete PV system and all its sources of energy losses, including inverter and transformer efficiency, wiring

resistance, clipping, soiling, and shading. Here we calculate specific yield using the same simulated energy production as for CSER, meaning none of these losses are considered and the resulting yield is thus an idealized representation of module performance. Because the specific yield values reported in this work are taken at the module level, they will be skewed high relative to the system-level values reported elsewhere.

III. RESULTS

A. HOW DOES PERFORMANCE VARY ACROSS CLIMATES AND PV MODULES?

First, we use the gridded NSRDB broadband irradiance, spectral irradiance, and meteorological data to quantify and characterize the climatic variation of module performance across the CONUS. Fig. 4 depicts maps of CSER and specific yield for each of the five PV modules. Fig. 5 depicts the distribution of CSER grouped by Köppen-Geiger climate zones.

For CSER, broad geographic/climatic trends are qualitatively similar across different modules, though the scale of variation differs by more than 10% across the CONUS. The highest CSER values, reaching up to 103%, are observed in the Upper Midwest, while the southern and southwestern regions show values as low as 86.2%. As shown in Fig. 5, this climatic/geographic variability is only partially described by KG climate zone. Variation in CSER is minimal within uniform climate zones like zone BWh (hot desert), while the range in zone Csb (warm summer Mediterranean) spans nearly the full range for all of CONUS. However, across all climates and modules, it is rare to achieve STC efficiency, with almost all locations having CSER below 100%. Comparing the CSER results across modules, we see that some modules show stronger climatic variation than others, but FSLRs4 consistently achieves the highest CSER across all climate zones, reaching a maximum median value of 99.3% in zones Dfa and Dfb. The four silicon-type modules show comparable results across CONUS as a whole, with median CSER varying by 1.5%, although differences are larger (up to 3%) for individual climate zones. Which of the four silicon modules is the best performer also depends on climate zone.

For yield, the geographic/climatic trends are also qualitatively similar across modules. However, the results reveal that yield is only loosely correlated with CSER. For example, all five modules have CSER roughly equal in regions of the southwest and southeast CONUS, while yield can vary by nearly 50% between the two regions. More broadly, we see that CSER variation (85–105%, or approximately $\pm 10\%$) is significantly smaller than yield variation (1500–3000 kWh/kW$_p$, or approximately $\pm 30\%$). Referring to Eq. 2 we see that the only difference between these two metrics is the solar resource, leading to the conclusion that variation in resource is roughly three times as important as variation in CSER when considering yield. We also note that locations with the highest yield (desert southwest) tend to also have lowest CSER, and that the FSLRs4 module's CSER

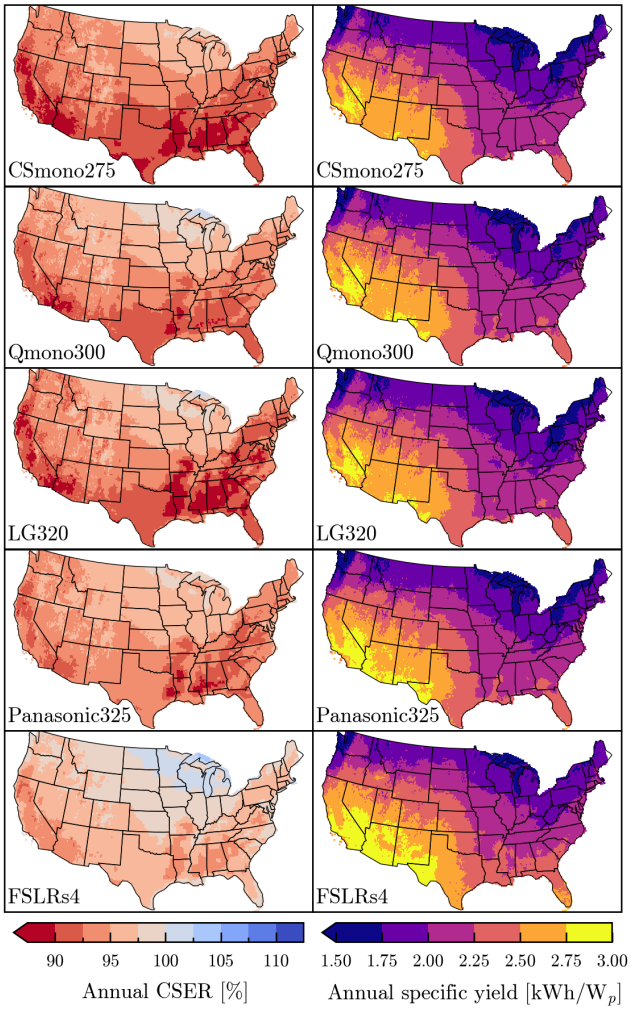

FIGURE 4. Geographic variation in annual CSER (left column) and specific yield (right column) for each module based on ∼20 km gridded irradiance and meteorological data from the NSRDB. With few exceptions, all modules perform worse (relative to STC) across CONUS. Geographic variation in CSER is only loosely correlated with variation in specific yield. Note that yield is calculated assuming single-axis tracking with no system losses.

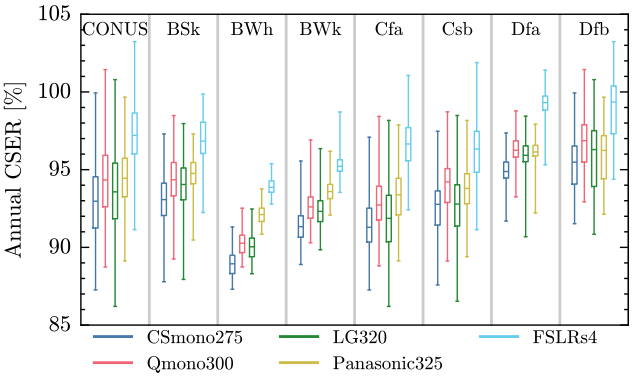

FIGURE 5. Distribution of annual CSER across the principal Köppen-Geiger climate zones in CONUS: BSk (cold semi-arid), BWh (hot desert), BWk (cold desert), Cfa (humid subtropical) Csb (warm-summer Mediterranean), Dfa (hot-summer continental), Dfb (warm-summer continental).

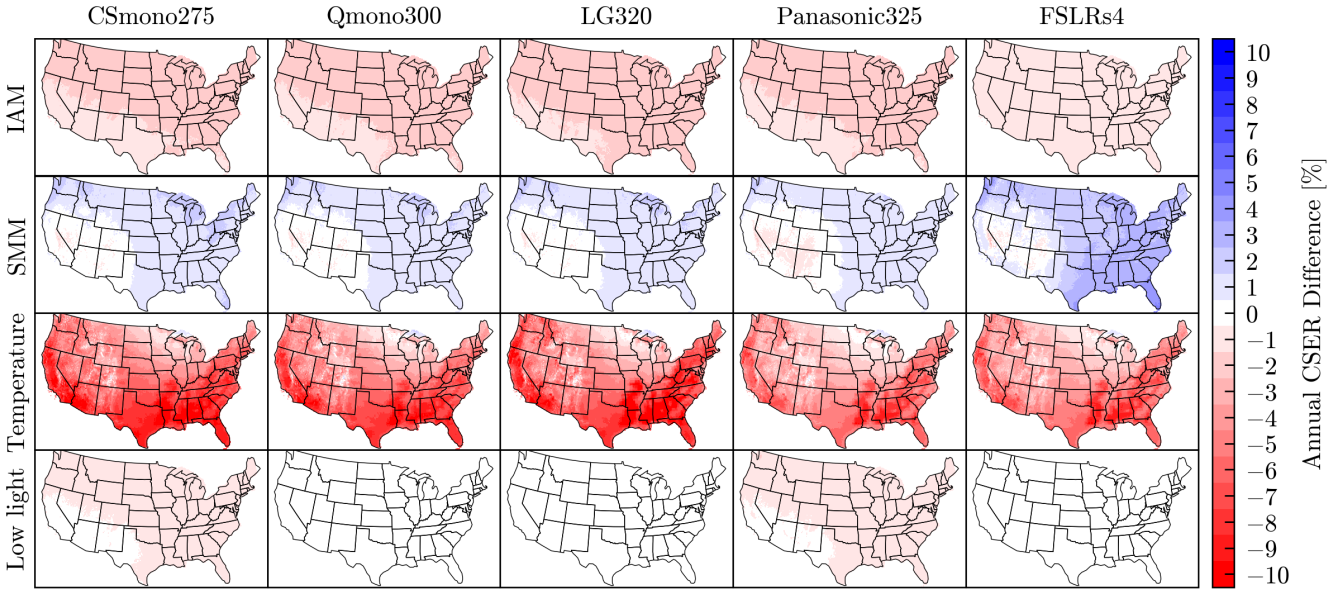

FIGURE 6. **Geographic variation of each aspect of module performance (incidence angle modifier (IAM), spectral mismatch (SMM), temperature, and low light. Color bands indicate unit ranges aligned to half-integers (e.g. white indicates the range from -0.5 to +0.5).**

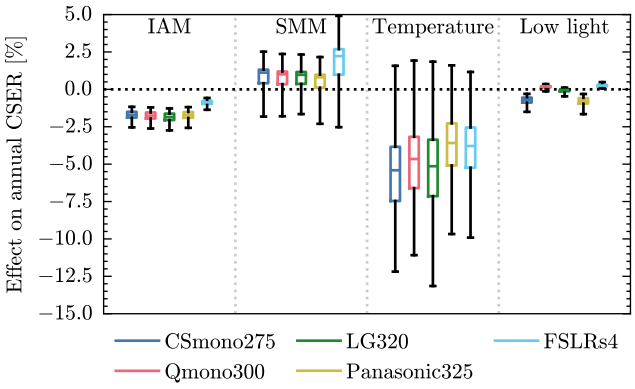

FIGURE 7. **The contribution of each performance effect to CSER across CONUS. The effects of temperature and spectrum are highly variable across climates, while IAM and low light are more consistent.**

advantage translates to a yield improvement of 2–6% over the silicon-type modules.

B. WHICH ASPECTS OF PV MODULE PERFORMANCE ARE THE PRIMARY SOURCES OF THE CSER VARIATION?

To determine and quantify the effects driving the CSER differences across modules and climates, specific module and cell characteristics were investigated: IAM, SMM, temperature, and low-light behavior. Fig. 6 shows how the contribution of each of these four PV performance aspects varies geographically. The same results are summarized in Fig. 7. Temperature has the most significant impact on the CSER ranging from -13.1% up to 1.9%. This means that, as expected, the temperature effect will typically negatively impact CSER, though not everywhere in the CONUS. Panasonic325 and FSLRs4 experience noticeably less temperature effect than the other modules do, consistent with the differences in temperature coefficient shown in Table 1. However, note that Qmono300 shows reduced temperature effect relative to LG320, despite the two modules having nearly identical temperature coefficients. This is due to differences in the thermal coefficients u_0 and u_1, meaning these often-overlooked coefficients can have meaningful impact on energy rating. Note that our simulations assume open racking; for roof-mount or building-integrated arrays, the temperature effect may be larger.

IAM remains nearly constant across different climates with a median impact of 1.7% for the silicon modules, making it the second-most influential factor in most locations. The advantageous IAM profile of FSLRs4 results in a reduced IAM loss of only 0.9%. For other racking configurations (e.g. fixed tilt and vertical), the effect of IAM may be larger.

The effect of spectral mismatch is variable, with gains of 0.5–1.5% being typical but some locations reaching 2.5% and 4.9% for silicon and CdTe, respectively. The four silicon modules show similar trends, with Panasonic325 showing a slightly reduced gain relative to the other three. The source of the geographic pattern was not investigated in this work.

Low-light conditions generally have a negligible impact; however, in certain climates and for specific modules, they can cause a marginal effect exceeding -1.5%. The calculated annual losses align well with expectations based on the low-light efficiency curves shown in Fig. 2; modules with more pronounced efficiency reduction at low light (CSmono275 and Panasonic325) experience larger low-light impact to CSER.

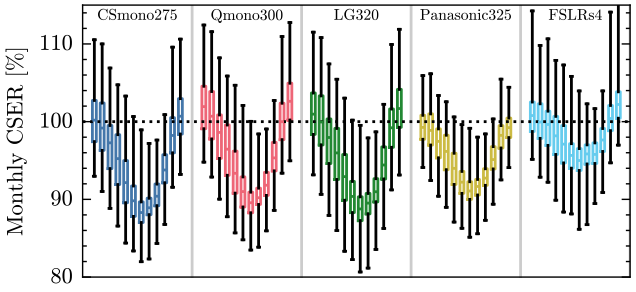

FIGURE 8. **Monthly CSER evaluated across CONUS. Each sequence of box-and-whiskers represents the months January through December. Geographic variation is comparable in scale to temporal variation.**

C. HOW DOES CSER VARY SEASONALLY?

CSER as defined in IEC 61853-3 is an annual metric, but we now calculate it on a monthly basis in order to evaluate seasonal variation in module efficiency. The calculation is identical except for consideration of only monthly subsets rather than the complete annual dataset. With each monthly subset, we also compute CSERs with each of the four aspects of performance held at STC as described previously.

Fig. 8 shows how CSER varies seasonally, with the individual contribution of each of the four performance effects shown in Fig. 9. Similar to the annual behavior, temperature is also the primary driver of CSER seasonality. Low-light losses are concentrated in the winter months, except for the FSLRs4 module, which performs up to 1% better under these conditions. The IAM also worsens in winter due to the simulated configuration (i.e., single-axis tracking). Qualitatively, among the analyzed modules, Panasonic325 exhibits the least geographic variation, while FSLRs4 shows the least seasonal variation. Notably, the seasonal effects tend to partially cancel each other out with IAM and low-light losses being balanced by temperature effects whereas for CdTe modules, the SMM offsets the temperature influences. The individual effects combined result in 7–13% seasonal variation, depending on the module, with all modules having winter CSER above 100% for some locations.

D. HOW DOES PARAMETER VALUE UNCERTAINTY AFFECT CSER?

To assess the effect of uncertainty in performance model parameters, CSER was recomputed using alternative parameter values for each module. In principle, this analysis could be applied to the parameters for all four performance effects considered in this work. Here we apply it to only the IAM and thermal parameters, as the test laboratory reports indicate the uncertainty, or provide alternative parameter values, for these parameters.

For IAM, the test reports for these modules provide a value and uncertainty for the Martin/Ruiz parameter a_r (e.g. $a_r = 0.1590 \pm 0.0018$). The stated uncertainties for these values are sufficiently small to produce no more than 0.1% variation in simulated performance. With such a small effect size, the

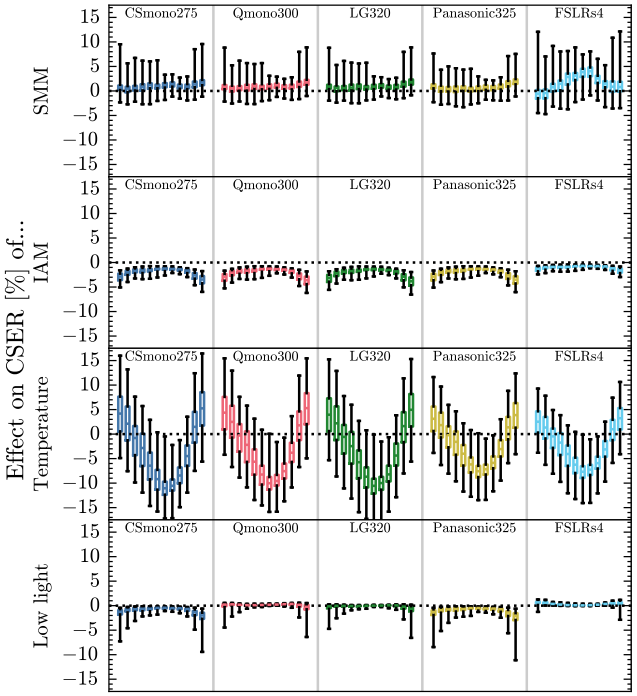

FIGURE 9. **Seasonal variation in the contribution of each performance effect to overall CSER. Each sequence of box-and-whiskers represents the months January through December.**

TABLE 2. **Alternative sets of Faiman thermal coefficients for each module, taken from the module characterization reports.**

Name	Set 1		Set 2	
	u_0	u_1	u_0	u_1
CSmono275	28.825	4.452	29.432	4.468
LG320	24.229	7.182	24.903	7.011
Panasonic325	24.614	7.878	28.657	5.983
Qmono300	30.536	5.019	30.280	5.071
FSLRs4	24.400	6.904	28.100	5.856

results are omitted here for brevity.

The test reports also indicate uncertainties for the Faiman thermal coefficients u_0 and u_1. However, they also offer a second set of values for u_0 and u_1 obtained by following a slightly modified data filtering procedure when fitting the empirical temperature measurements. The two sets of parameter values for each module are listed in Table 2. Because the two sets of parameter values were fitted to similar datasets using similar techniques, they give a rough indication of real-world parameter estimation variability, and it is thus informative to compare the CSERs resulting from each set.

Fig. 10 shows the difference in annual specific yield between the two sets of u_0 and u_1 values. The difference varies significantly across the five modules, with CSmono275 and Qmono300 showing less than 0.25% difference and Panasonic325 and FSLRs4 showing larger differences of up to 1.5%. Additionally, a geographic pattern is evident, where large differences in annual yield occur in regions with low

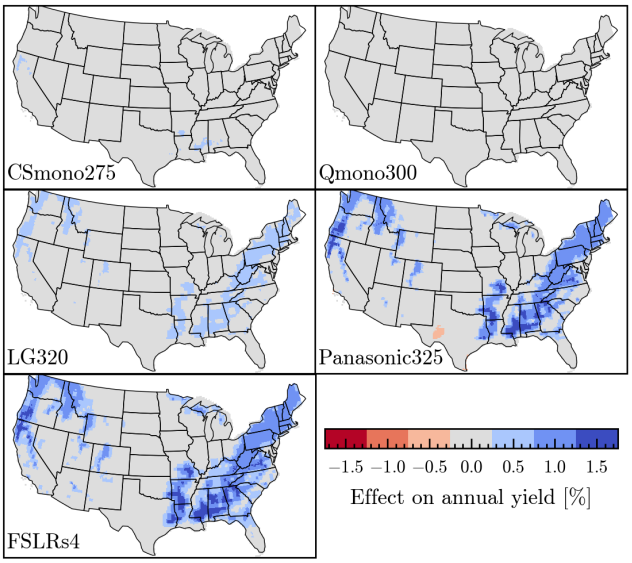

FIGURE 10. Difference in simulated annual yield resulting from using alternative values for the Faiman thermal coefficients u_0 and u_1. The effect size varies significantly with both module and location/climate.

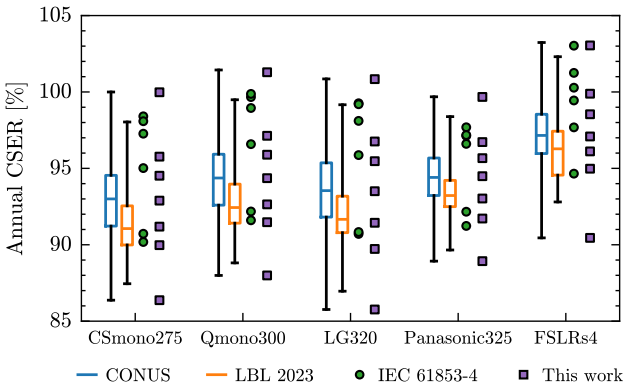

FIGURE 11. Comparison of CSER distributions for four sets of locations: the full contiguous United States (CONUS), the current locations of deployed utility-scale PV systems (LBL 2023), the six IEC 61853-4 reference datasets, and the seven locations proposed in this work. The CSER distribution for the reference datasets is shifted high relative to the distributions for CONUS and LBL 2023, while the proposed locations accurately reflect the CONUS distribution.

annual wind speed (according to the weather dataset used in the simulation).

E. ARE THE IEC 61853-4 CLIMATIC DATASETS REPRESENTATIVE OF THE CONUS?

To assess whether the six IEC 61853-4 [24] reference climates are representative of the climatic conditions across the CONUS, we compare the CSER results from these different datasets to each other (see Fig. 11). In addition, to avoid representing systems that are unrealistic (e.g., on the peak of a tall mountain), Fig. 11 also compares against CSER values from locations of 1258 real utility-scale PV power plants taken from the 2023 utility scale solar report from Lawrence Berkeley Lab (LBL) [40].

Overall, we can see that the IEC 61853-4 climatic datasets tend to over-estimate CSER in the CONUS. To quantify these differences, average CSERs for each of these three sets of locations are provided in Table 3. Relative to the CSER for CONUS, the CSER corresponding to the locations of real PV systems is 0.9–1.6% lower on average. We also see that the IEC 61853-4 reference datasets skew high relative to the distributions of both CONUS and LBL 2023 (1.0–2.2% and 1.9–3.7% on average, respectively), resulting in the lower tails of these distributions extending significantly below the minimum CSER of the reference datasets. The fraction of locations with CSER below the minimum reference CSER, for various regions, is shown in Fig. 12. We see that approximately 25% of locations of real PV systems, and roughly 10% of the entire CONUS, correspond to CSERs outside the range of CSER from the IEC 61853-4 reference datasets. Notably, for four out of the five modules, the majority of locations in the BWh (hot desert) climate zone have CSER outside the range of the IEC 61853-4 reference datasets. CSER for these

TABLE 3. Mean CSER values for different regions of the United States. CSER values are given in percent.

	CONUS	LBL 2023	IEC 61853-4
CSmono275	92.9	91.4	94.9
Qmono300	94.3	92.7	96.5
LG320	93.5	92.0	95.7
Panasonic325	94.4	93.4	95.3
FSLRs4	97.2	96.2	99.4

unrepresented locations fall as much as 5% below the lowest CSER for the reference datasets.

Motivated by these observations, we present a set of alternative reference datasets (or rather, their locations and NSRDB statistics) that more accurately represent the distribution of CSER across CONUS. These locations were chosen by identifying locations in the full set of CSER simulations that, across the five modules, most closely matched a range of seven target CSER percentiles from 0 (lowest CSER in CONUS) to 100 (highest CSER in CONUS). Details for the seven locations are listed in Table 4, and shown graphically in Figs. 11 and 13. Unlike the IEC 61853-4 reference datasets, the proposed set of locations accurately represents the CONUS CSER distribution, including the lower tail. Finally, we note that as CSER percentile increases, annual GHI decreases, annual average temperature decreases, and wind speed increases.

IV. DISCUSSION AND CONCLUSION

The CSmono275, Qmono300, and LG320 modules exhibit similar behavior across climates, whereas the Panasonic325 and FSLRs4 modules demonstrate distinct performance characteristics. These characteristics are due to the low temperature coefficients combined with the unique low-light SHJ behavior and the spectral impact on CdTe modules. The FSLRs4 module demonstrated the highest CSER, and thus

TABLE 4. Proposed reference locations for PV module energy rating. Columns indicates the nominal CSER percentile ("Target"), the location coordinates ("Latitude" and "Longitude"), climatic parameters (annual global horizontal irradiation, "GHI"; annual direct normal irradiation, "DNI"; annual average ambient temperature, T_{amb}; annual average wind speed, W_{spd}), and the actual CSER percentiles for each of the five modules.

Target %	Latitude °	Longitude °	GHI MWh/m^2	DNI MWh/m^2	T_{amb} °C	W_{spd} m/s	CSmono275 %	FSLRs4 %	LG320 %	Panasonic325 %	Qmono300 %
0	36.49	-118.90	1.99	2.44	20.94	0.55	0.00	0.00	0.00	0.00	0.00
10	33.69	-83.90	1.75	2.00	17.05	0.60	9.76	12.29	7.49	7.90	10.65
25	36.49	-93.50	1.71	2.07	14.53	1.23	24.54	27.79	20.18	21.42	25.75
50	46.69	-120.50	1.59	2.05	10.31	1.56	48.18	48.69	49.56	51.75	49.87
75	46.09	-109.10	1.48	1.80	7.66	3.25	74.50	75.00	76.48	74.85	74.46
90	42.69	-90.10	1.46	1.74	8.10	3.37	89.42	90.47	90.04	90.66	89.40
100	47.89	-87.30	1.19	1.16	3.00	5.57	100.00	99.99	100.00	100.00	99.99

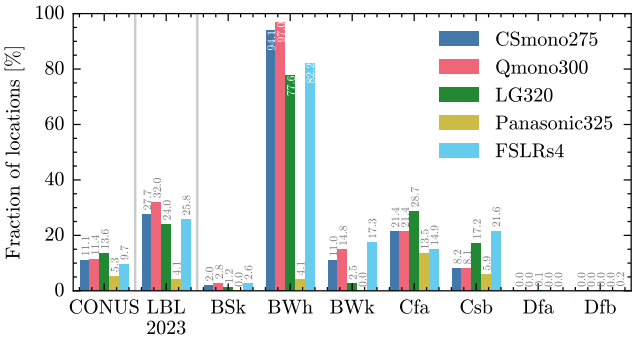

FIGURE 12. Fraction of locations where CSER falls below the minimum CSER calculated for the IEC 61853-4 reference datasets.

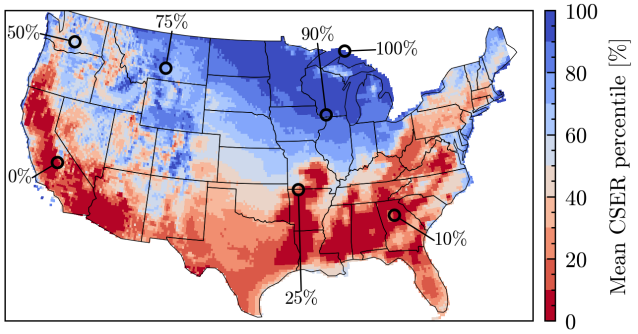

FIGURE 13. Map of the proposed reference locations. Color indicates CSER percentile averaged across the five modules.

yield, due to its advantageous performance across all four key effects including a favorable spectral mismatch and low-light response, reduced IAM loss, and lower temperature-related losses.

Thermal effects were found to have the largest impact (up to 12.5%) on CSER in most climates. Either IAM or spectral mismatch was the next largest effect (up to 2.5% and 5% for IAM and spectral effects, respectively), depending on location. However, the effect of low-light response is generally marginal. The module with the most pronounced low-light effect, the Panasonic325 module, exhibits a relative efficiency reduction to 90% at 100 Wm^{-2}, translating to an annual loss of only approximately 1%. However, all four effects are amplified in some times of year due to seasonality, although seasonality in IAM and low-light response tends to partially cancel out seasonality in thermal effects.

Secondary performance differences originate from the thermal coefficients u_0 and u_1, whose uncertainty was found to affect simulated CSER by up to 1.5%. Notably, the uncertainty in these coefficient values is comparable in scale to the variation between modules. Based on this finding, we identify a need for improved parameter estimation methods for the u_0 and u_1 parameters.

Additionally, the IEC 61853-4 reference datasets do not represent the full range of climates where PV systems are currently deployed. For example, in the high solar resource and high temperature region of southwestern Arizona, the irradiance-weighted ambient temperature is 31°C while the hottest IEC 61853-4 dataset has only 26.4°C. This highlights that the IEC 61853-4 reference datasets do not represent the full range of conditions in the CONUS, and in particular the regions of CONUS with highest solar resource. However, a proposed new set of reference locations, identified based on CSER directly rather than climate type, much more accurately represents the full distribution of CSER across the CONUS.

A primary limitation of this work is that the results are based on a single year of data (2022), which introduces the potential for the results to be affected by interannual variation. On the other hand, similar to TMYs, the IEC 61853-4 climate datasets are intended to provide a representative weather file, which might not capture all anomalies or variations occurring in a single year. This work is also limited in that, due to lack of required data, it considers only monofacial modules, while PV deployment continues to shift towards bifacial technologies. Additionally, module degradation, metastability effects, and other real-world operational issues are not considered. Furthermore, the CSER values reflect efficiency at maximum power point (MPP), and do not take into account additional losses such as clipping and soiling. These effects (which are also not considered in IEC 61853-3) would have a significant impact on system-level energy yield.

Future work should evaluate the effects of recent and future advances in PV module technology, including bifaciality, half-cut and shingled cells, and new cell types like TOPCon and perovskites. Publicly available characterization datasets

for these module technologies would be of great value to such work. Additionally, alternative installation types such as floating PV and building-integrated PV are known to have differing thermal characteristics and could also be evaluated in this context. Finally, projected datasets from climate models could be used to estimate how PV performance will shift over time due to climate change.

DATA AVAILABILITY

The data supporting the findings of this study will be made available upon publication through the PV Atlas website, a project led by the PV Performance Modeling Collaborative (PVPMC): https://sandialabs.github.io/pv-atlas/

The PV module characterization datasets used in this work are available on the PVPMC website: https://pvpmc.sandia.gov/datasets/

ACKNOWLEDGMENT

The authors thank the NREL NSRDB team, especially Yu Xie, for kindly supplying the gridded spectral irradiance data used in this work. The authors also thank two anonymous reviewers for their valuable feedback.

Sandia National Laboratories is a multimission laboratory managed and operated by National Technology & Engineering Solutions of Sandia, LLC, a wholly owned subsidiary of Honeywell International Inc., for the U.S. Department of Energy's National Nuclear Security Administration under contract DE-NA0003525. This paper describes objective technical results and analysis. Any subjective views or opinions that might be expressed in the paper do not necessarily represent the views of the U.S. Department of Energy or the United States Government.

REFERENCES

[1] T. Huld and A. Amillo, "Estimating PV module performance over large geographical regions: The role of irradiance, air temperature, wind speed and solar spectrum," *Energies*, vol. 8, no. 6, p. 5159–5181, Jun. 2015. [Online]. Available: http://dx.doi.org/10.3390/en8065159

[2] "Photovoltaic (PV) module performance testing and energy rating - Part 3: Energy rating of PV modules," International Electrotechnical Commission, Standard 61853-3:2018, 2018.

[3] "Climatic rating of photovoltaic modules: Different technologies for various operating conditions," IEA PVPS Task 13, Report T13-20, 2020.

[4] K. Kawajiri, T. Oozeki, and Y. Genchi, "Effect of temperature on PV potential in the world," *Environmental Science & Technology*, vol. 45, no. 20, p. 9030–9035, Sep. 2011. [Online]. Available: http://dx.doi.org/10.1021/es200635x

[5] J. Polo, M. Alonso-Abella, J. A. Ruiz-Arias, and J. L. Balenzategui, "Worldwide analysis of spectral factors for seven photovoltaic technologies," *Solar Energy*, vol. 142, p. 194–203, Jan. 2017. [Online]. Available: http://dx.doi.org/10.1016/j.solener.2016.12.024

[6] G. S. Kinsey *et al.*, "Impact of measured spectrum variation on solar photovoltaic efficiencies worldwide," *Renewable Energy*, vol. 196, p. 995–1016, Aug. 2022. [Online]. Available: http://dx.doi.org/10.1016/j.renene.2022.07.011

[7] A. Amillo, T. Huld, P. Vourlioti, R. Müller, and M. Norton, "Application of satellite-based spectrally-resolved solar radiation data to PV performance studies," *Energies*, vol. 8, no. 5, p. 3455–3488, Apr. 2015. [Online]. Available: http://dx.doi.org/10.3390/en8053455

[8] D. Dirnberger, G. Blackburn, B. Müller, and C. Reise, "On the impact of solar spectral irradiance on the yield of different PV technologies," *Solar Energy Materials and Solar Cells*, vol. 132, p. 431–442, Jan. 2015. [Online]. Available: http://dx.doi.org/10.1016/j.solmat.2014.09.034

[9] J. M. Ripalda, D. Chemisana, J. M. Llorens, and I. García, "Location-specific spectral and thermal effects in tracking and fixed tilt photovoltaic systems," *iScience*, vol. 23, no. 10, p. 101634, Oct. 2020. [Online]. Available: http://dx.doi.org/10.1016/j.isci.2020.101634

[10] M. Alonso-Abella, F. Chenlo, G. Nofuentes, and M. Torres-Ramírez, "Analysis of spectral effects on the energy yield of different PV (photovoltaic) technologies: The case of four specific sites," *Energy*, vol. 67, p. 435–443, Apr. 2014. [Online]. Available: http://dx.doi.org/10.1016/j.energy.2014.01.024

[11] M. Schweiger and W. Herrmann, "Comparison of energy yield data of fifteen PV module technologies operating in four different climates," in *2015 IEEE 42nd Photovoltaic Specialist Conference (PVSC)*. IEEE, Jun. 2015. [Online]. Available: http://dx.doi.org/10.1109/PVSC.2015.7356123

[12] A. Louwen, A. C. de Waal, R. E. I. Schropp, A. P. C. Faaij, and W. G. J. H. M. van Sark, "Comprehensive characterisation and analysis of PV module performance under real operating conditions," *Progress in Photovoltaics: Research and Applications*, vol. 25, no. 3, p. 218–232, Dec. 2016. [Online]. Available: http://dx.doi.org/10.1002/pip.2848

[13] J. Y. Ye, T. Reindl, A. G. Aberle, and T. M. Walsh, "Effect of solar spectrum on the performance of various thin-film PV module technologies in tropical Singapore," *IEEE Journal of Photovoltaics*, vol. 4, no. 5, p. 1268–1274, Sep. 2014. [Online]. Available: http://dx.doi.org/10.1109/JPHOTOV.2014.2328585

[14] T. Huld, R. Gottschalg, H. G. Beyer, and M. Topič, "Mapping the performance of PV modules, effects of module type and data averaging," *Solar Energy*, vol. 84, no. 2, p. 324–338, Feb. 2010. [Online]. Available: http://dx.doi.org/10.1016/j.solener.2009.12.002

[15] T. Huld, M. Šúri, and E. D. Dunlop, "Geographical variation of the conversion efficiency of crystalline silicon photovoltaic modules in Europe," *Progress in Photovoltaics: Research and Applications*, vol. 16, no. 7, p. 595–607, Jul. 2008. [Online]. Available: http://dx.doi.org/10.1002/pip.846

[16] H. Nguyen and J. Pearce, "Estimating potential photovoltaic yield with r.sun and the open source geographical resources analysis support system," *Solar Energy*, vol. 84, no. 5, p. 831–843, May 2010. [Online]. Available: http://dx.doi.org/10.1016/j.solener.2010.02.009

[17] ESMAP, "Global photovoltaic power potential by country," World Bank Group, Report 149846, 2020. [Online]. Available: http://documents.worldbank.org/curated/en/466331592817725242/Global-Photovoltaic-Power-Potential-by-Country

[18] I. M. Peters, H. Liu, T. Reindl, and T. Buonassisi, "Global prediction of photovoltaic field performance differences using open-source satellite data," *Joule*, vol. 2, no. 2, p. 307–322, Feb. 2018. [Online]. Available: http://dx.doi.org/10.1016/j.joule.2017.11.012

[19] S. Lindig, M. Herz, J. Ascencio-Vásquez, M. Theristis, B. Herteleer, J. Deckx, and K. Anderson, "Review of technical photovoltaic key performance indicators and the importance of data quality routines," *Solar RRL*, Nov. 2024. [Online]. Available: http://dx.doi.org/10.1002/solr.202400634

[20] J. Ascencio-Vásquez, K. Brecl, and M. Topič, "Methodology of Köppen-Geiger-photovoltaic climate classification and implications to worldwide mapping of PV system performance," *Solar Energy*, vol. 191, p. 672–685, Oct. 2019. [Online]. Available: http://dx.doi.org/10.1016/j.solener.2019.08.072

[21] M. Theristis, K. Anderson, J. Ascencio-Vásquez, and J. S. Stein, "How climate and data quality impact photovoltaic performance loss rate estimations," *Solar RRL*, Dec. 2023. [Online]. Available: http://dx.doi.org/10.1002/solr.202300815

[22] J. Ascencio-Vásquez, I. Kaaya, K. Brecl, K. A. Weiss, and M. Topič, "Global climate data processing and mapping of degradation mechanisms and degradation rates of PV modules," *Energies*, vol. 12, no. 24, p. 4749, Dec. 2019. [Online]. Available: http://dx.doi.org/10.3390/en12244749

[23] W. Herrmann, C. Monokroussos, and K. Lee, "Comparison of different approaches to determine the nominal PV module operating temperature (NMOT)," in *38th European Photovoltaic Solar Energy Conference*, 2021.

[24] "Photovoltaic (PV) module performance testing and energy rating - Part 4: Standard reference climatic profiles," International Electrotechnical Commission, Standard 61853-4:2018, 2018.

[25] M. Rivera, C. Reise, and U. Kräling, "Representativeness of energy rating acc. to IEC 61853 for different locations in middle and south Europe," *Energy Technology*, vol. 11, no. 12, Jun. 2023. [Online]. Available: http://dx.doi.org/10.1002/ente.202300356

[26] M. Sengupta, Y. Xie, A. Lopez, A. Habte, G. Maclaurin, and J. Shelby, "The national solar radiation data base (NSRDB)," *Renewable and*

Sustainable Energy Reviews, vol. 89, pp. 51–60, Jun. 2018. [Online]. Available: https://doi.org/10.1016/j.rser.2018.03.003

[27] F. Rubel and M. Kottek, "Observed and projected climate shifts 1901-2100 depicted by world maps of the Köppen-Geiger climate classification," *Meteorologische Zeitschrift*, vol. 19, no. 2, p. 135–141, Apr. 2010. [Online]. Available: http://dx.doi.org/10.1127/0941-2948/2010/0430

[28] Y. Xie and M. Sengupta, "A fast all-sky radiation model for solar applications with narrowband irradiances on tilted surfaces (FARMS-NIT): Part I. the clear-sky model," *Solar Energy*, vol. 174, p. 691–702, Nov. 2018. [Online]. Available: http://dx.doi.org/10.1016/j.solener.2018.09.056

[29] Y. Xie, M. Sengupta, and C. Wang, "A fast all-sky radiation model for solar applications with narrowband irradiances on tilted surfaces (FARMS-NIT): Part II. the cloudy-sky model," *Solar Energy*, vol. 188, p. 799–812, Aug. 2019. [Online]. Available: http://dx.doi.org/10.1016/j.solener.2019.06.058

[30] J. Stein, "PV performance modeling and stakeholder engagement (Q3 FY2020 project report)," Sandia National Laboratories, Tech. Rep. SAND-2020-8325R, Jul. 2020. [Online]. Available: http://dx.doi.org/10.2172/1647906

[31] "PVPMC: PV lifetime module characterization datasets and reports," https://pvpmc.sandia.gov/datasets/pv-lifetime-module-datasets, accessed: 2024-05-24.

[32] "Third party validation of First Solar PAN files," First Solar, Tech. Rep. PD-5-500 rev 2.0, 2016.

[33] A. Driesse, M. Theristis, and J. Stein, "Global horizontal spectral irradiance and module spectral response measurements: an open dataset for PV research," Sandia National Laboratories, Tech. Rep. SAND2023-02045, 2023. [Online]. Available: http://dx.doi.org/10.21948/2204677

[34] W. F. Holmgren, C. W. Hansen, and M. A. Mikofski, "pvlib python: a python package for modeling solar energy systems," *Journal of Open Source Software*, vol. 3, no. 29, p. 884, Sep. 2018. [Online]. Available: http://dx.doi.org/10.21105/joss.00884

[35] K. S. Anderson, C. W. Hansen, W. F. Holmgren, A. R. Jensen, M. A. Mikofski, and A. Driesse, "pvlib python: 2023 project update," *Journal of Open Source Software*, vol. 8, no. 92, p. 5994, Dec. 2023. [Online]. Available: http://dx.doi.org/10.21105/joss.05994

[36] pvlib-python contributors, "pvlib/pvlib-python: v0.11.0," 2024. [Online]. Available: https://zenodo.org/doi/10.5281/zenodo.12209694

[37] A. Driesse and J. Stein, "From IEC 61853 power measurements to PV system simulations," Sandia National Laboratories, Tech. Rep. SAND-2020-3877, Apr. 2020. [Online]. Available: http://dx.doi.org/10.2172/1615179

[38] A. Driesse, M. Theristis, and J. S. Stein, "A new photovoltaic module efficiency model for energy prediction and rating," *IEEE Journal of Photovoltaics*, vol. 11, no. 2, p. 527–534, Mar. 2021. [Online]. Available: http://dx.doi.org/10.1109/JPHOTOV.2020.3045677

[39] R. Vogt *et al.*, "PV module energy rating standard IEC 61853-3 intercomparison and best practice guidelines for implementation and validation," *IEEE Journal of Photovoltaics*, vol. 12, no. 3, p. 844–852, May 2022. [Online]. Available: http://dx.doi.org/10.1109/JPHOTOV.2021.3135258

[40] M. Bolinger, J. Seel, J. Kemp, C. Warner, A. Katta, and D. Robson, "Utility-scale solar, 2023 edition: Empirical trends in deployment, technology, cost, performance, PPA pricing, and value in the United States," Lawrence Berkely National Laboratory, Tech. Rep., Oct. 2023. [Online]. Available: http://dx.doi.org/10.2172/2007458

KEVIN S. ANDERSON received B.S. degrees in physics and applied mathematics from the University of North Carolina, Chapel Hill, in 2016.

He is a Senior Member of the Technical Staff with the Sandia National Laboratories, Photovoltaics and Materials Technology Department. His research interests include PV performance modeling and monitoring, solar tracker modeling and optimization, and open-source software. Prior to joining the Sandia National Laboratories, he was a researcher at the National Renewable Energy Laboratory from 2019 to 2023. He has also worked in the solar energy industry monitoring and optimizing utility-scale PV system performance.

MARIOS THERISTIS received the Dipl.-Ing. degree in electrical and computer engineering from the Democritus University of Thrace, Greece, in 2011, and the Ph.D. degree from Heriot-Watt University, U.K., in 2016.

He is a Principal Member of the Technical Staff with the Sandia National Laboratories, Photovoltaics and Materials Technology Department, where he is the Principal Investigator of the PV performance modeling and PV O&M analytics programs. Prior to joining the Sandia National Laboratories, he was with the University of Cyprus, Cyprus, from 2016 to 2019, the University of Jaén, Spain, in 2016, the Fraunhofer CSE, USA, in 2015, and the NCSR "Demokritos," Greece, from 2010 to 2011.

JOSHUA S. STEIN received the Ph.D. degree in earth sciences from the University of California, Santa Cruz, in 2000.

He joined Sandia, in 2001, where he is currently a Senior Scientist. He currently leads research and development projects in the areas of photovoltaic module and system performance and reliability, specializing in modeling and analysis of new technologies. He is the Founder of the PV Performance Modeling Collaborative, represents the USA in the International Energy Agency PVPS Task 13 on PV Performance and Reliability, and is the Director of the Perovskite PV Accelerator for Commercial Technologies (PACT). He has over 200 publications.